Ocean Sci. Discuss., 12, 2283–2313, 2015
www.ocean-sci-discuss.net/12/2283/2015/
doi:10.5194/osd-12-2283-2015

Ocean Science
Discussions
Open Access

Remote sensing of chlorophyll in the Baltic Sea at basin scale from 1997 to 2012 using merged multisensor data

J. Pitarch[1], **G. Volpe**[1], **S. Colella**[1], **H. Krasemann**[2], **and R. Santoleri**[1]

[1]Institute for Climate and Atmospheric Sciences, Italian National Research Council, Via del Fosso del Cavaliere 100, 00133 Rome, Italy
[2]Helmholtz-Zentrum Geesthacht, Centre for Materials and Coastal Research GmbH, Max-Planck-Strasse 1, 21502 Geesthacht, Germany

Received: 9 September 2015 – Accepted: 10 September 2015 – Published: 30 September 2015

Correspondence to: J. Pitarch (jaime.pitarchportero@artov.isac.cnr.it)

Published by Copernicus Publications on behalf of the European Geosciences Union.

Abstract

Fifteen-year (1997–2012) time series of chlorophyll *a* (CHL) in the Baltic Sea, based on merged multisensor satellite data provided by the European projects Globcolour and ESA-OC-CCI were analysed. Several available CHL algorithms were sea-truthed against a large in situ CHL dataset consisting of data by Seadatanet, HELCOM and NOAA. Matchups were calculated for three separate areas (1) Skagerrak and Kattegat, (2) Baltic Proper plus gulfs of Riga and Finland, called here "Central Baltic", (3) Gulf of Bothnia, and for the three areas as a whole. Statistics showed low linearity. The OC4v6 algorithm (R^2 = 0.46, BIAS = +60 %, RMS = 79 % for the whole dataset) was linearly transformed by using the best linear fit (OC4corr). By construction, the bias was corrected, but RMS was increased instead. Despite this shortcoming, we demonstrated that errors between OC4corr and in situ data were log-normally distributed and centred at zero. Consequently, unbiased estimators of the horizontally-averaged CHL could be obtained, the error of which tends to zero when a large amount of pixels is averaged. From the basin-wide time series, the climatology and the annual anomalies were separated. The climatologies revealed completely different CHL dynamics among regions: in Skagerrak and Kattegat, CHL strongly peaks in late winter, with a minimum in summer and a secondary peak in spring. In the Central Baltic, CHL follows a dynamics of a spring CHL peak, followed by a much stronger summer bloom, with decreasing CHL towards winter. The Gulf of Bothnia shows a similar CHL dynamics as the central Baltic, although the summer bloom is absent. Across years, CHL showed great variability. Supported by auxiliary satellite sea-surface temperature (SST) data, we found that phytoplankton growth was inhibited in the central Baltic Sea in the years of colder summers or when the SST happened to increase later in the season. Extremely high CHL in spring 2008 was detected and linked to an exceptionally warm preceding winter. Sharp SST changes were found to induce CHL changes in the same direction. This phenomenon was appreciated best by overlaying the time series of the CHL and SST anomalies.

OSD

12, 2283–2313, 2015

1 Introduction

The limits of oceans and seas are set and revised in a series of documents by the International Hydrographic Organization (IHO), the last version of which (IHO, 1953) sets the border between the Baltic Sea and the North Sea south of the three straits of Little Belt, Great Belt and Øresund, thus leaving the Skagerrak and Kattegat, at the north side of the Danish archipelago, out of the Baltic Sea. However, the Baltic Marine Environment Protection Commission – Helsinki Commission (HELCOM) defines in its Article 1 the "Baltic Sea Area" as the Baltic Sea and the entrance to the Baltic Sea bounded by the parallel of the Skaw in the Skagerrak at 57°44.43′ N, thus including the Kattegat, but leaving the Skagerrak out its domain (HELCOM, 1992). On the other hand, the European Commission's Copernicus Marine environment monitoring service (CMEMS, follow-on of the MyOcean project) provides operational monitoring products over the world's oceans, with emphasis on European seas. In view of a new specific "Baltic area" chlorophyll *a* (CHL) product, the eastern limit has been set at the meridian 9.24° E, thus including most of the Skagerrak.

In this article, we are interested in the Copernicus-defined Baltic area as a whole, given that a single CHL algorithm is going to be implemented in the operational processing chain. Thus statistics should be consequently calculated. Nevertheless, although no bio-optical measurements in the Baltic area are publicly available, we expect the bio-optics of different regions to be substantially different. Water salinity is more than 30 psu north of the Danish Straits and about ∼ 7 psu in the Baltic Proper, whereas it decreases to almost 0 northwards when entering the Bothnian Bay. In Summer, cyanobacteria blooms are commonly observed in the Baltic Proper but not in the Skagerrak and Kattegat and the Gulf of Bothnia (Wasmund and Uhlig, 2003). In Skagerrak and Kattegat, the phytoplankton dynamics is expected to be different than the rest of the Baltic.

Satellite-borne medium resolution ocean colour sensors offer an excellent possibility to monitor phytoplankton dynamics at daily or near-daily frequencies. In the liter-

OSD
12, 2283–2313, 2015

ature, applications of remote sensing in the Baltic Sea have been mainly focused on few main topics: cyanobacteria blooms (Reinart and Kutser, 2006), light penetration (Pierson et al., 2008) and management of various coastal areas (Kratzer et al., 2008), to cite a few. A good overview of such different applications is found in Siegel and Gerth (2008). Long-term data series have been much less analysed. Here, the works of M. Kahru and collaborators are worth citing. They used long-term multisensor satellite data to develop an indicator of surface cyanobacterial accumulation over defined Baltic regions and searched for trends (Kahru and Elmgren, 2014; Kahru et al., 2007). However, there is a lack of studies of long-term phytoplankton dynamics over large areas, despite the fact that the regular monitoring of phytoplankton is required by the European Water Framework Directive for coastal and inland waters and by the Marine Strategy Framework Directive for open ocean waters. In this article, we aim to partially fill this gap by focusing on long-term remote sensing of CHL at basin-wide scale. This task is subject to a number of issues in the Baltic Sea: atmospheric correction is problematic at blue wavelengths due to low remote-sensing reflectance (R_{rs}) (Mélin and Vantrepotte, 2015). Absorption in the blue is dominated by CHL-uncorrelated dissolved substances, which can mask CHL absorption (Berthon et al., 2008). Suspended sediment concentration can be high in shallow and semi-enclosed areas, which interferes with CHL retrieval.

Coincident in situ measurements are needed to complement and help interpret the remote-sensing signal. Despite the fact that the Baltic Sea is widely recognized to be a challenging test bed for remote sensing, literature on calibration/validation of CHL is not abundant. Application of several Standard MODIS and SeaWiFS algorithms to in situ R_{rs} revealed a mean CHL bias $> 100\,\%$ with respect to in situ CHL (Darecki and Stramski, 2004), using data at 707 stations off Poland between 1993 and 2001. In a following paper (Darecki et al., 2005), best linear fits were used to produce new unbiased SeaWiFS algorithms. It was also shown that these algorithms tend to lose sensitivity for CHL around or below $1\,\mathrm{mg\,m^{-3}}$ (their Fig. 10). Worse results were obtained when four standard CHL algorithms were applied to SeaWiFS images between

OSD
12, 2283–2313, 2015

2000 and 2001 (HELCOM, 2004, Fig. 4.4). Matchup to 75 CHL profiles across all the Baltic Sea, with predominance of Swedish coastal waters, gave almost no correlation. Moreover, satellite CHL underestimated the in situ CHL by 180 to 500 %, in contradiction with Darecki and Stramski (2004). Recently, the Case 2 Regional, Boreal, and Eutrophic processors were applied to MERIS images between 2006 and 2009 (Attila et al., 2013). Matchup at 312 stations in the Gulf of Finland and the central Baltic Sea showed great CHL overestimation. When the default bio-optical relationships of these processors were tuned with the in situ CHL, the bias seemed to reduce significantly (their Fig. 6). Bias calculations were not presented though.

Ocean colour has cloud cover as additional problem, which is particularly high over northern Europe. To increase the spatial coverage of daily products, the International Ocean-Colour Coordinating Group (IOCCG) recommended the merging of ocean colour data from multiple missions (IOCCG, 2007). At European level, the ESA-OC-CCI (www.esa-oceancolour-cci.org) and Globcolour (www.globcolour.info) projects followed the former recommendation and reprocessed archived data from various medium-resolution sensors. The EU CMEMS program provides satellite, in situ and modelling data for the European Seas and the global ocean. For specific seas, CMEMS applies regional algorithms to CCI-derived daily R_{rs}, except for the Baltic Sea, over which a validated product is still missing and users can only refer to the global product (MyOcean, 2014).

In this article, we process multisensor, merged and consistently inter-calibrated satellite CHL daily data for the period 1997–2012, over the Baltic area. For calibration and validation of available CHL algorithms, an extensive, publicly available in situ CHL dataset is used. Algorithms are tested in these four geographical areas: (1) Skagerrak and Kattegat, (2) Baltic Proper plus gulfs of Riga and Finland, called here "central Baltic", (3) Gulf of Bothnia, and (4) the total area (1 to 3) as a whole. Thus, we evaluate several algorithms that are usable to estimate CHL using merged satellite data, with the inherent limitation of using only the SeaWiFS bands. A second outcome of this article is to obtain reliable CHL horizontal averages when unbiased estimators are derived from

OSD
12, 2283–2313, 2015

any of these pre-existing algorithms, despite the low correlation. When calculated on a daily basis for such a long time range (1997–2012), the obtained data is of a unique value to study the ecology of the Baltic area and its regions in a synoptic scale. To our understanding, this kind of time series data remains up to date undocumented.

2 Data

2.1 Satellite CHL data

The GlobColour dataset was developed in the framework of the European Space Agency Data User Element program to support global carbon cycle research. Daily GlobColour data are available on the web site www.globcolour.info. Products are obtained by merging MERIS, MODIS, SeaWiFS and VIIRS data. Validation at global scale was carried out by Maritorena et al. (2010). Downloaded data are newly-produced 2nd reprocessing Level 3 binned images (L3b), having a resolution of $1/24^\circ$ at the equator (i.e., around 4.63 km) and consisting of the accumulated data of all merged level 2 products, corresponding to periods of one day (a data-day algorithm is applied). Merged data are generated by the GSM model (Maritorena and Siegel, 2005), which also produces the CHL parameter, delivered as product named CHL1. GlobColour declare their "CHL1" parameter (GLC here) as applicable only in case 1 waters, but no alternative is given for the Baltic Sea. For further details, the reader is referred to GlobColour (2015).

The ESA Ocean Colour Climate Change Initiative project (CCI) has the goal to provide stable, long-term, multisensor satellite products. The dataset merges SeaWiFS, MODIS, and MERIS data, and shifts the resulting R_{rs} to the SeaWiFS wavebands, before merging (ESA-OC-CCI, 2014). Data are mapped at 4 km resolution and are available through the OC-CCI portal (www.oceancolour.org) and also through the MyOcean portal (www.myocean.eu). Standard CHL products are global-ocean daily mean sea surface CHL, named OCEAN-

OSD
12, 2283–2313, 2015

COLOUR_GLO_CHL_L3_REP_OBSERVATIONS_009_065. ESA-CCI retrieves CHL through application of the OC4v6 algorithm (O'Reilly et al., 2000; Werdell, 2010) to the merged R_{rs}. The MyOcean dataset includes an additional CHL product by applying the OC5 algorithm (Gohin et al., 2002), developed as an adaptation of the OC4 to French coastal waters. See (MyOcean, 2014, p.21) for details. Calibrated R_{rs} are also available under the name OCEAN-COLOUR_GLO_OPTICS_L3_REP_OBSERVATIONS_009_064, for the application of custom algorithms. We used these R_{rs} to test a Baltic Sea-specific CHL algorithm, available for the SeaWiFS bands, developed by D'Alimonte et al. (2011). This algorithm is based on a Multi-layer perceptron (MLP) and was calibrated with in situ R_{rs} and CHL. Posteriorly, it was only validated (D'Alimonte et al., 2012) with in situ R_{rs} and CHL.

Table 1 lists the satellite CHL products evaluated in this article with their respective references. An image pre-analysis revealed many more flagged (invalid) pixels for MLP than for OC4v6 and OC5, despite being derived from the same CCI reflectances. The cause is the frequent occurrence of negative R_{rs} (412) due to aerosol optical thickness overestimation in the blue together with high CDOM. In contrast, OC4v6 does not use R_{rs} (412), the most sensible band to the atmospheric correction procedure, thus allowing for problematic pixels (those with $R_{rs}(412) < 0$) to be retrieved as well. In the context of being able to retrieve CHL also under extreme conditions, e.g., atmospheric correction failure, OC5 does accept negative R_{rs} (412).

2.2 Auxiliary satellite SST data

To investigate the relationship between CHL dynamics and temperature, we downloaded reprocessed daily-averaged sea-surface temperature (SST) from 1997 until 2009 on the Baltic Sea from the MyOcean website, product named SST_BAL_SST_L4_REP_OBSERVATIONS_010_016. The product is merged and quality-controlled data from sensors NOAA AVHRRs 7, 9, 11, 14, 16, 17, 18, Envisat ATSR1, ATSR2 and AATSR. See MyOcean (2013) for further information.

OSD
12, 2283–2313, 2015

2.3 In situ CHL data

Publicly available in situ CHL databases are managed by the Seadatanet project (www.seadatanet.org), the Baltic Marine Environment Protection Commission (www.helcom.fi) and the NOAA's World Ocean Database (www.nodc.noaa.gov/OC5/WOD/pr_wod.html). In all databases, quality, compatibility and coherence of the data issuing from many sources is assured by the adoption of standardized methodologies. All data collected in the Baltic area during the period covered by the satellite observations (1997–2012) were downloaded, merged and duplicates were eliminated. Only CHL values with the quality flag equal to zero (accepted value) were considered.

CHL consisted either of a single sub-surface reading or CHL profiles derived from a few depth readings. In this latter case, a proper vertical average of a CHL profile is needed for comparison to remote-sensing data. The vertical weighting function depends on the inherent optical properties (IOPs) that cannot be inferred solely from CHL in case 2 waters. In rigor, coincident IOP measurements are needed to perform the vertical averaging, but such measurements are scarce and not publicly available. In case 1 waters, vertical averaging can be performed with the method by Morel and Berthon (1989) with input CHL profile data. The remaining applicable options to our in situ data were either to select only the sub-surface CHL value or to average the profiles with the method by Morel and Berthon (1989), despite the theoretical inconsistencies. Preliminary calculations (not shown) revealed that correlation improved slightly if available profiles were vertically averaged instead of taking only the uppermost reading. Therefore, we decided to proceed with this approach for the rest of the article. To avoid bottom contribution to the water-leaving radiance, only stations with a bottom depth of at least 10 m were selected. Similarly, to ensure representativeness of the data in the case of CHL stratification, only stations with the uppermost reading not deeper than 2 m were retained for the analysis. For comparison issues among algorithms, only matchups with coincident valid pixels for all four satellite products within the same day were considered, but once the best performing algorithm was identified, all available

OSD
12, 2283–2313, 2015

matchup stations for this algorithm were used. Satellite CHL was extracted from single pixels without spatial windowing. The spatial distribution of sampling stations is shown in Fig. 1. They distribute over the whole area but are not uniformly mapped, as the dataset is built from different sources, in which individual institutes and agencies are interested in particular zones. For instance, a high agglomeration of stations at the entrance of the Gulf of Finland could suggest a higher relative weight of this specific area in the statistics.

3 Results

3.1 Matchups

Both in situ and satellite CHL distributions were approximately log-normal (not shown). Consequently, we applied decimal logarithm-transformation to the CHL data to calculate the mean bias and the RMS, and returned to percentage linear scale, as shown in Eqs. (1) and (2):

$$\mathrm{BIAS} = \left[10^{\frac{1}{N}\sum_{i=1}^{N}(y_i - x_i)} - 1\right] \cdot 100 \quad (1)$$

$$\mathrm{RMS} = \left[10^{\frac{1}{N}\sqrt{\sum_{i=1}^{N}(y_i - x_i)^2}} - 1\right] \cdot 100, \quad (2)$$

where x_i and y_i are the $\log_{10}$-transformed in situ and satellite CHL, respectively. N is the number of matchups. The coefficient of determination R^2 was computed using the log-transformed CHL. The slope (m) and the intercept (n) of the best linear fits are also presented.

Outliers were defined as the stations in which any of the four all algorithms gave CHL outside the range within 1/20 and 20 times the in situ CHL. In applying this criterion, ~ 3.5 % of the data was discarded and led to N = 1873. The whole area was divided into regions with expected bio-optical differences (see Fig. 1). These are: (1) Skarregat

OSD
12, 2283–2313, 2015

and Kattegat (N = 622), (2) Central Baltic (N = 1212) and (3) Gulf of Bothnia (N = 39). Figure 2 presents all density scatter plots and statistics in condensed form. The data available for the Gulf of Bothnia is very limited, so the statistical information that it can be derived from the regressions must be interpreted with caution. Nevertheless, results are also presented there for completeness. The p value of the regressions was zero for all except for the Gulf of Bothnia, where it was $p < 10^{-3}$.

For the whole dataset, agreement between satellite and in situ data is modest in general. MLP and GLC provide poor R^2 and some negative BIAS respect to the in situ data. Results of OC4v6 (R^2 = 0.43) are consistent with findings by Darecki and Stramski (2004). The positive bias of 44 % here (Fig. 2o) is smaller than their 119 %, but still confirms a high overestimation of CHL in Baltic waters. OC4v6 matches better the in situ data for high CHL, whereas tends to saturate for low CHL. OC5 has similar linearity (R^2 = 0.44) and lowers the overestimated CHL by OC4v6 (Gohin et al., 2002), leading here to some overcompensation (−14 %). Besides the similar R^2, we appreciated graphical similarities between the scatter plots of OC4v6 and OC5. Guided by this hint, we performed a linear regression in log form between OC4v6 and OC5 satellite derived CHL (not shown). Regression analysis revealed a very high linear dependence (R^2 = 0.97), although the relationship is more complex in theory (Gohin et al., 2002).

Geographical partition of the matchup dataset highlighted significant differences in the statistical behaviour of algorithms. For instance, the performance of MLP strongly degrades in Skagerrak and Kattegat respect to the Baltic Sea. MLP was calibrated with data only inside the Baltic Sea, and not in the Skagerrak and Kattegat (D'Alimonte et al., 2012, Fig. 2d). It appears then that such algorithm design is highly dependent on the calibration data. GLC performs always worst in all regions, and the scatter plots seem like undefined clouds, which is best highlighted by the great RMS errors. OC4v6 displays similar statistics at both sides of the Danish Strait, although the regression line is somewhat more horizontal for Skagerrak and Kattegat. In all cases, OC4v6 overestimates CHL more than 40 %. The behaviour of OC5 is always in accordance to OC4v6, with a shifted BIAS, given the very high correlation between both. Due to the

OSD
12, 2283–2313, 2015

much simpler applicability of OC4v6 and its wider diffusion in the community, we chose to perform calculations hereafter only for OC4v6.

Next, the matchup analysis is repeated with the same conditions, but now for OC4v6 alone, regardless of other algorithms at any given station. When this constraint is removed, the matchup stations increase for the whole dataset up to $N = 4492$, which divides into $N = 1456$ in Skagerrak and Kattegat, $N = 2922$ in the Central Baltic and $N = 114$ in the Gulf of Bothnia. Figure 3 shows the corresponding density scatter plots and statistics. The interpretation from Fig. 2 holds also here, but the bigger size of the matchup dataset adds increased confidence in the derived statistics.

3.2 Validation

When the regression coefficients are to be used for linear re-calibration of existing algorithms, the validity and robustness of the matchup statistics need to be validated against independent data. Starting from the matchups for OC4v6 alone, (Fig. 3d) we performed a sensitivity study on the homogeneity by a bootstrapping like assessment (Efron, 1979) as used in recent validation exercises (Brewin et al., 2015). The whole dataset ($N = 4492$) was partitioned a thousand times into two randomly chosen halves: calibration ($N_{cal} = 2246$) and validation ($N_{val} = 2246$). The obtained series of coefficients (m, n) are plotted in Fig. 4, left. Results are remarkably robust: the averages of the regressions found ($m = 0.5843$, $n = 0.3657$, green dashed) are almost equal to those when the whole dataset is used ($m = 0.5845$ and $n = 0.3656$, red). Moreover, the dispersion is very small with the coefficient of variation of the slopes being 2.07 % and for the intercepts 1.38 %. We then applied each calibration of Fig. 4, left to the corresponding complementary validation datasets and plotted the resulting series of statistics in Fig. 4, right. Their mean values (in green) $R^2 = 0.4236$, BIAS = 59.55 %, RMS = 136.13 % are very similar to those obtained for the whole dataset (Fig. 3d, $R^2 = 0.4241$, BIAS = 59.53 %, RMS = 136.19 %).

OSD
12, 2283–2313, 2015

Consequently, the coefficients calculated with the calibration datasets (Fig. 4) were used to recalibrate OC4v6 with e Eq. (3):

$$\log_{10}(\mathrm{CHL}_{\mathrm{OC4v6corr}}) = \frac{\log_{10}(\mathrm{CHL}_{\mathrm{OC4v6}}) - n}{m}. \quad (3)$$

Errors between Eq. (3) and the complementary in situ validation matchups were calculated. Each of the 1000 chosen combinations generated a vector of errors with length $N_{\mathrm{val}} = 2246$. Their accumulation led to a total of 2 246 000 error estimates, whose distribution is shown in Fig. 5, together with the fitted Gaussian curve. It is shown that the recalibration via Eq. (3) removed the bias, resulting in a zero-centred error distribution; it is worth reminding that the calibration and validation datasets are independent. The standard deviation ($\sigma = 0.4582$) includes all errors not taken into account by the system, i.e. atmospheric noise, limited performance of OC4v6 and errors in the in situ measurements.

3.3 Satellite derived basin averages and discussion

The symmetric and zero-centred error distribution obtained with $\mathrm{OC4v6_{corr}}$ in Fig. 5 warrants a high confidence when basin averages are calculated, since all the errors on individual pixel level are expected to cancel out when a horizontal (pixel-wise) average is performed over a big region. Although the former statement implies that the statistical properties of our matchup dataset can be extrapolated to the whole Baltic area, the good spatial and temporal coverage of the former (see Fig. 1) is a good asset to support this argument. From this point, we defined the algorithm $\mathrm{OC4v6_{corr}}$ through Eq. (3), with the coefficients $(m, n) = (0.5884, 0.3751)$ of Fig. 3d. This enabled the bias to be removed, while keeping the same R^2. Nevertheless, RMS was altered, rising up to 187 %, in agreement with $\sigma = 0.4582$ in Fig. 5 through Eq. (2). The mathematical explanation of the latter relationship is that the RMS and the standard deviation of a zero-mean distribution are equal.

OSD
12, 2283–2313, 2015

It has been nevertheless acknowledged in Fig. 3 that the best linear fits are different among regions in the Baltic area. If OC4v6 is linearly adjusted with Eq. (3), the coefficients must be different for each region, in particular, equal to those found in Fig. 3. Therefore, for Skagerrak and Kattegat, we set $(m, n) = (0.4212, 0.3027)$. Due to the lack of enough data in the Gulf of Bothnia, we aggregated its stations to the Central Baltic data. The resulted statistics for these two regions were almost equal to those of the Central Baltic alone: $R^2 = 0.35$, BIAS = 60.45 %, RMS = 138.64 %, $(m, n) = (0.5632, 0.4206)$. These linear coefficients were applied to recalibrate OC4v6 for the Central Baltic and Gulf of Bothnia. Despite using the same algorithm, results are presented separately for both basins.

Horizontal-averaged CHL for $OC4v6_{corr}$ were computed only for images with a minimum number of 1000 valid pixels. A posterior 3 days moving median was applied to remove spikes. Results are shown for each region and for the entire domain, in Fig. 6. During the years when only SeaWiFS was operating, data gaps are more frequent, especially in Skagerrak and Kattegat. This fact further highlights the benefit of using merged data when available. A first glimpse of the plot shows several events with too high CHL in early Spring in Skagerrak and Kattegat. The reason for this result is the following: many OC4v6 images in early Spring contained areas with CHL $> 10\,mg\,m^{-3}$, but very few of our matchups reflect this phenomenon (Fig. 3a). Causes could be the relatively sharp temporal occurrence of these late winter high CHL events and a less frequent in situ sampling at that time of the year. When applying the regression coefficients of Eq. (3), the CHL values at the right end of Fig. 3a are excessively risen. These values CHL $> 10\,mg\,m^{-3}$ in Skagerrak and Kattegat are not reliable because they lay outside the range for algorithm training. Additionally, it is worth rising the awareness that in this region, eventual coccolithophore blooms are not optimally detected with a blue-green algorithm like OC4v6 (Gordon et al., 2001). Contrariwise, the training range in the Central Baltic (Fig. 3b) covered well the range of the time series, so the mentioned problem did not appear there. However, few spikes in the time series were

OSD
12, 2283–2313, 2015

caused by images whose valid pixels were predominantly over the Gulfs of Riga and Finland, thus overestimating the mean CHL for the whole region.

Data in Fig. 6 shows different dynamics among regions. Skagerrak and Kattegat show a higher CHL dynamics in late winter and a minimum towards summer, whereas at the other side of the Danish Strait, the dynamics seems opposite. To better appreciate these phenomena, we calculated the climatologies as the inter-annual averages. For any given day of the year, the average was computed only if data for a minimum of six years were available. Results are shown in Fig. 7. In Skagerrak and Kattegat, the dynamics consists of intermittent growth periods in late winter and a much flatter dynamics from spring, reaching a minimum in summer. In the Central Baltic, the dynamics is completely different. Two distinct CHL maxima are appreciable: the first one peaks at the end of April, reaching $\sim 2.3\,\mathrm{mg\,m^{-3}}$ and the second one peaks in mid-July with $\sim 3.9\,\mathrm{mg\,m^{-3}}$, from which it decreases steadily and reaches the minimum in winter. In the Gulf of Bothnia, the dynamics is similar to that of the Central Baltic, showing minimum CHL in winter and a spring bloom. The summer blooms appear absent in our data, and mean CHL remains around $\sim 2\,\mathrm{mg\,m^{-3}}$. Nevertheless, the latter time series has to be interpreted with caution due to lack of a significant number of data for specific calibration. Moreover, the Gulf of Bothnia is normally ice-covered in winter, and some ice remains in the northern part until May. Displayed CHL belongs to ice-free areas. Finally, the mean CHL of the entire domain (including Skagerrak and Kattegat) is displayed. The dynamics is clearly dominated by the Central Baltic and Gulf of Bothnia, due to its major weight when spatial averages are computed. When winter approaches, mean CHL decreases, with slightly higher values than the Central Baltic and Gulf of Bothnia, due to the higher influence of Skagerrak and Kattegat.

A complementary time series of basin-averaged SST is depicted in Fig. 8. High SST are known to enhance the growth of cyanobacteria, both directly through higher growth rates, and indirectly by increasing the stability of the water column to allow cyanobacteria to take advantage of their buoyancy regulation ability (Ibelings et al., 1991). Figure 9 shows the CHL and SST anomalies in the central Baltic with respect to

OSD
12, 2283–2313, 2015

their climatologies, concentrated in the summer period. The CHL anomaly time series has been further smoothed with a one-week moving average. The figure shows quite a surprising relationship between both quantities, that is, high-amplitude temperature anomalies induce similar growth and decay in CHL. This related behaviour is somewhat unexpected, because we are comparing here not absolute CHL and temperature, but their differences with respect to their climatological values. In almost all years, positive temperature anomalies seemed to trigger strong blooms, and sudden SST decreases induced also decreases in CHL.

This article is focused on the remote sensing aspect and the causes of these dynamics are undoubtedly complex. Nevertheless, we make here short comments on plausible explanations. Cyanobacterial growth is known to be favoured by high summer temperatures. The intensity of the cyanobacterial bloom appears to depend on the timing of the summer temperature peak: although 2004 had a high SST peak, such peak happened late in the season (10 August), which appeared not favourable for cyanobacteria growth. On the contrary, years 2002, 2003, 2005 and 2006 had SST peaks of similar or lower intensity, but much earlier in the season. Instead, 2001 displayed two marked positive SST anomalies that were only mildly followed by the CHL anomaly. Years 2010, 2011 and 2012 remained outside the SST series. However, the very marked CHL peak in summer 2010 has been reported in mass-media (BBC, 2010).

In 1998, no link between CHL and SST anomalies was apparent. That year, summer was abnormally cold (see Figs. 8 and 9). We argue that, in this case, CHL depended on the absolute temperature values rather than on the anomalies, perhaps through indirect factors like mixing. On the other hand, the year 2008 was completely anomalous with respect to both the climatology value and timing of the summer bloom, with a maximum at the beginning of May. This massive and early bloom has already been documented (Larsson et al., 2014; Majaneva et al., 2012), with the dominant species being *Prymnesium polylepis*. Responsible abiotic factors were exceptionally calm and sunny weather during October 2007, resulting in high light availability and low turbulence above the thermocline. These conditions enabled *P. polylepis* to build up a considerable biomass.

OSD
12, 2283–2313, 2015

The following winter (see also Figs. 8 and 9) was the mildest since more than a century, which allowed *P. polylepis* to persist throughout the winter. Improving weather and plenty of nutrients allowed further growth until a maximum in spring.

4 Conclusions

Fifteen years-long merged multisensor daily CHL data contains very valuable information for ecological studies if information is properly processed. Matchup analysis was undertaken with a large in situ database. Despite poor statistics of OC4v6 (R^2 = 0.42), we were able to calibrate an unbiased estimation for basin-averaged CHL. The $OC4v6_{corr}$-derived climatology in Skagerrak and Kattegat revealed strong productivity in late winter, towards a rather inactive summer, with the awareness that coccolitophore detection with a blue-green CHL algorithm is not optimal. In the Central Baltic, a first growth period with a maximum at the end of April was detected, followed by a stronger summer bloom peaking at the second week of July. Productivity in late fall, winter and early spring was severely inhibited. In the Gulf of Bothnia, the dynamics was similar as in the Central Baltic, but with the absence of a summer bloom. Significant annual deviations as compared with the climatology were related to anomalies in the SST annual excursion: cold summers limited cyanobacteria growth and warm summers favoured it. Cyanobacteria growth seemed to be enhanced by early summer SST peaks and hampered in correspondence of late-summer SST maxima. The exceptionally warm winter in 2008 triggered an intense spring bloom that also altered the normal dynamics throughout the year.

This study showed that accurate observations of averaged large areas can be performed with a high-RMS yet unbiased estimator. However, if observations are to be focused or partitioned into smaller areas, algorithms with higher R^2 are desirable. The interfering CDOM at blue wavelengths and adverse atmospheric conditions suggest that better CHL algorithms should move towards red and NIR bands, like a fluorescence line height or maximum chlorophyll index algorithms (Odermatt et al., 2012,

OSD
12, 2283–2313, 2015

Fig. 1). The CHL values found here (~ 1 to 5 mg m^{-3}) are at the lower part of the retrievable concentrations. Such algorithms are only applicable to the archived MERIS data (2002–2012). The Ocean and Land Colour Instrument, on-board and Sentinel-3 will provide continuity to MERIS data.

CHL is an aggregated marker of eutrophication, which is present in all phytoplankton. The oscillating patterns of CHL reported in this article are formed by different species whose proportions vary across both space and time. The discrimination of the individual dynamics of several functional groups, pigments or taxons from remote-sensing data would be an important added value to the observations. The achievement of this goal would depend on the sensitivity of the satellite-measured radiance to variations in several key pigments.

Our analysis provides a good confidence level about ocean colour retrieval over the Baltic Sea, even if it does not allow the ecological cause-effect relationship to be unequivocally derived. To address it, extensive chemical (organic and inorganic nutrients) and physical oceanographic conditions, other than bio-optical measurements should be routinely undertaken and in case assimilated into ecological models together with refined ocean colour observations.

The Supplement related to this article is available online at doi:10.5194/osd-12-2283-2015-supplement.

Acknowledgements. The research leading to these results has received funding from the European Union Seventh Framework Programme (FP7/2007-2013) under grant agreement no. 218812 (MyOcean project). Seadatanet, HELCOM and NOAA are thanked for the in situ data and GlobColour for the satellite data. V. Forneris is thanked for technical support and V. Brando for suggestions on the manuscript.

OSD
12, 2283–2313, 2015

References

Attila, J., Koponen, S., Kallio, K., Lindfors, A., Kaitala, S., and Ylöstalo, P.: MERIS Case II water processor comparison on coastal sites of the northern Baltic Sea, Remote Sens. Environ., 128, 138–149, 2013.

BBC: Satellite spies vast algal bloom in Baltic Sea, available at: http://www.bbc.co.uk/news/science-environment-10740097 (last access: 11 June 2015), 2010.

Berthon, J. F., Mélin, F., and Zibordi, G.: Ocean colour remote sensing of the optically complex European Seas, in: Remote Sensing of the European Seas, edited by: Barale, V. and Gade, M., Springer, Dordrecht, the Netherlands, 30–52, 2008.

Brewin, R. J. W., Sathyendranath, S., Müller, D., Brockmann, C., Deschamps, P.-Y., Devred, E., Doerffer, R., Fomferra, N., Franz, B., Grant, M., Groom, S., Horseman, A., Hu, C., Krasemann, H., Lee, Z., Maritorena, S., Mélin, F., Peters, M., Platt, T., Regner, P., Smyth, T., Steinmetz, F., Swinton, J., Werdell, J., and White Iii, G. N.: The Ocean Colour Climate Change Initiative: III. A round-robin comparison on in-water bio-optical algorithms, Remote Sens. Environ., 162, 271–294, doi:10.1016/j.rse.2013.09.016, 2015.

D'Alimonte, D., Zibordi, G., Berthon, J. F., Canuti, E., and Kajiyama, T.: Bio-Optical Algorithms for European Seas: Performance and Applicability of Neural-Net Inversion Schemes, Joint Research Centre, Ispra, Italy, JRC66326, 2011.

D'Alimonte, D., Zibordi, G., Berthon, J.-F., Canuti, E., and Kajiyama, T.: Performance and applicability of bio-optical algorithms in different European seas, Remote Sens. Environ., 124, 402–412, 2012.

Darecki, M. and Stramski, D.: An evaluation of MODIS and SeaWiFS bio-optical algorithms in the Baltic Sea, Remote Sens. Environ., 89, 326–350, 2004.

Darecki, M., Kaczmarek, S., and Olszewski, J.: SeaWiFS ocean colour chlorophyll algorithms for the southern Baltic Sea, Int. J. Remote Sens., 26, 247–260, 2005.

Efron, B.: Bootstrap methods: another look at the jackknife, Ann. Stat., 7, 1–26, 1979.

ESA-OC-CCI: Ocean Colour Climate Change Initiative (OC_CCI) – Phase One, Product User Guide, available at: http://www.esa-oceancolour-cci.org/?q=webfm_send/318 (last access: 11 June 2015), 2014.

GlobColour: GlobColour, Product User Guide, available at: http://www.globcolour.info/CDR_Docs/GlobCOLOUR_PUG.pdf last access: 11 June, 2015.

OSD
12, 2283–2313, 2015

Gohin, F., Druon, J. N., and Lampert, L.: A five channel chlorophyll concentration algorithm applied to SeaWiFS data processed by SeaDAS in coastal waters, Int. J. Remote Sens., 23, 1639–1661, 2002.
Gordon, H. R., Boynton, G. C., Balch, W. M., Groom, S. B., Harbour, D. S., and Smyth, T. J.: Retrieval of coccolithophore calcite concentration from SeaWiFS Imagery, Geophys. Res. Lett., 28, 1587–1590, 2001.
HELCOM: Convention on the Protection of the Marine Environment of the Baltic Sea Area, available at: http://www.helcom.fi/about-us/convention/ (last access: 11 June 2015), 1992.
HELCOM: Thematic Report on Validation of Algorithms for Chlorophyll a Retrieval from Satellite Data in the Baltic Sea Area, Helsinki Commission-HELCOM, Ispra, 94, 2004.
Ibelings, B. W., Mur, L. R., and Walsby, A. E.: Diurnal changes in buoyancy and vertical distribution in populations of Microcystisin two shallow lakes, J. Plankton Res., 13, 419–436, 1991.
IHO: Limits of Oceans and Seas, International Hydrographic Organization, PANGAEA, Bremerhaven, Germany, 1953.
IOCCG: Ocean-Colour Data Merging, 13 December 2006, IOCCG, Dartmouth, Canada, 72 pp., 2007.
Kahru, M. and Elmgren, R.: Multidecadal time series of satellite-detected accumulations of cyanobacteria in the Baltic Sea, Biogeosciences, 11, 3619–3633, doi:10.5194/bg-11-3619-2014, 2014.
Kahru, M., Savchuk, O. P., and Elmgren, R.: Satellite measurements of cyanobacterial bloom frequency in the Baltic Sea: interannual and spatial variability, Mar. Ecol.-Prog. Ser., 343, 15–23, 2007.
Kratzer, S., Brockmann, C., and Moore, G.: Using MERIS full resolution data to monitor coastal waters – a case study from Himmerfjärden, a fjord-like bay in the northwestern Baltic Sea, Remote Sens. Environ., 112, 2284–2300, 2008.
Larsson, K., Hajdu, S., Kilpi, M., Larsson, R., Leito, A., and Lyngs, P.: Effects of an extensive Prymnesium polylepis bloom on breeding eiders in the Baltic Sea, J. Sea Res., 88, 21–28, 2014.
Majaneva, M., Rintala, J.-M., Hajdu, S., Hällfors, S., Hällfors, G., Skjevik, A.-T., Gromisz, S., Kownacka, J., Busch, S., and Blomster, J.: The extensive bloom of alternate-stage Prymnesium polylepis (Haptophyta) in the Baltic Sea during autumn–spring 2007–2008, Eur. J. Phycol., 47, 310–320, 2012.

OSD
12, 2283–2313, 2015

Maritorena, S. and Siegel, D. A.: Consistent merging of satellite ocean color data sets using a bio-optical model, Remote Sens. Environ., 94, 429–440, 2005.
Maritorena, S., d'Andon, O. H. F., Mangin, A., and Siegel, D. A.: Merged satellite ocean color data products using a bio-optical model: characteristics, benefits and issues, Remote Sens. Environ., 114, 1791–1804, 2010.
Mélin, F. and Vantrepotte, V.: How optically diverse is the coastal ocean?, Remote Sens. Environ., 160, 235–251, 2015.
Morel, A. and Berthon, J.-F.: Surface pigments, algal biomass profiles, and potential production of the euphotic layer: relationships reinvestigated in view of remote-sensing applications, Limnol. Oceanogr., 34, 1545–1562, 1989.
MyOcean: Product User Manual for all Ocean Colour Products, available at: http://catalogue.myocean.eu.org/static/resources/myocean/pum/MYO2-OC-PUM-009-ALL-V1.0.pdf (last access: 15 June 2015), 2014.
MyOcean: Product User Manual For Baltic Sea Physical Reanalysis Products, available at: http://catalogue.myocean.eu.org/static/resources/myocean/pum/MYO2-BAL-PUM-003-004-005-V1.2.pdf (last access: 15 June 2015), 2013.
O'Reilly, J. E., Maritorena, S., O'Brien, M. C., Siegel, D. A., Toole, D., Menzies, D., Smith, R. C., Mueller, J. L., and Kahru, M.: Ocean color chlorophyll a algorithms for SeaWiFS, OC2, and OC4: Version 4. SeaWiFS Postlaunch Calibration and Validation Analyses, in: NASA Technical Memorandum, NASA Goddard Space Flight Center, Greenbelt, Maryland, USA, 1–49, 2000.
Odermatt, D., Gitelson, A., Brando, V. E., and Schaepman, M.: Review of constituent retrieval in optically deep and complex waters from satellite imagery, Remote Sens. Environ., 118, 116–126, 2012.
Pierson, D. C., Kratzer, S., Strömbeck, N., and Håkansson, B.: Relationship between the attenuation of downwelling irradiance at 490 nm with the attenuation of PAR (400 nm–700 nm) in the Baltic Sea, Remote Sens. Environ., 112, 668–680, 2008.
Reinart, A. and Kutser, T.: Comparison of different satellite sensors in detecting cyanobacterial bloom events in the Baltic Sea, Remote Sens. Environ., 102, 74–85, 2006.
Siegel, H. and Gerth, M.: Optical remote sensing applications in the Baltic Sea, in: Remote Sensing of the European Seas, edited by: Barale, V. and Gade, M., Springer, Dordrecht, the Netherlands, 91–102, 2008.

OSD
12, 2283–2313, 2015

Wasmund, N. and Uhlig, S.: Phytoplankton trends in the Baltic Sea, ICES J. Mar. Sci., 60, 177–186, 2003.
Werdell, P. J.: Ocean Color Chlorophyll (OC) v6, available at: http://oceancolor.gsfc.nasa.gov/REPROCESSING/R2009/ocv6/ (last access: 15 June 2015), 2010.

OSD
12, 2283–2313, 2015

Table 1. List of satellite CHL products analysed in this article.

Acronym	Description
MLP	L3 ESA CCI daily merged SeaWiFS/MODIS/MERIS. MLP algorithm (D'Alimonte et al., 2011)
GLC	L3b GlobColour daily merged SeaWiFS/MODIS/MERIS/VIIRS. GSM algorithm (Maritorena and Siegel, 2005)
OC4v6	L3 ESA CCI daily merged SeaWiFS/MODIS/MERIS. OC4v6 algorithm (O'Reilly et al., 2000). Updated in Werdell (2010)
OC5	L3 ESA CCI daily merged SeaWiFS/MODIS/MERIS. OC5 algorithm (Gohin et al., 2002)

OSD
12, 2283–2313, 2015

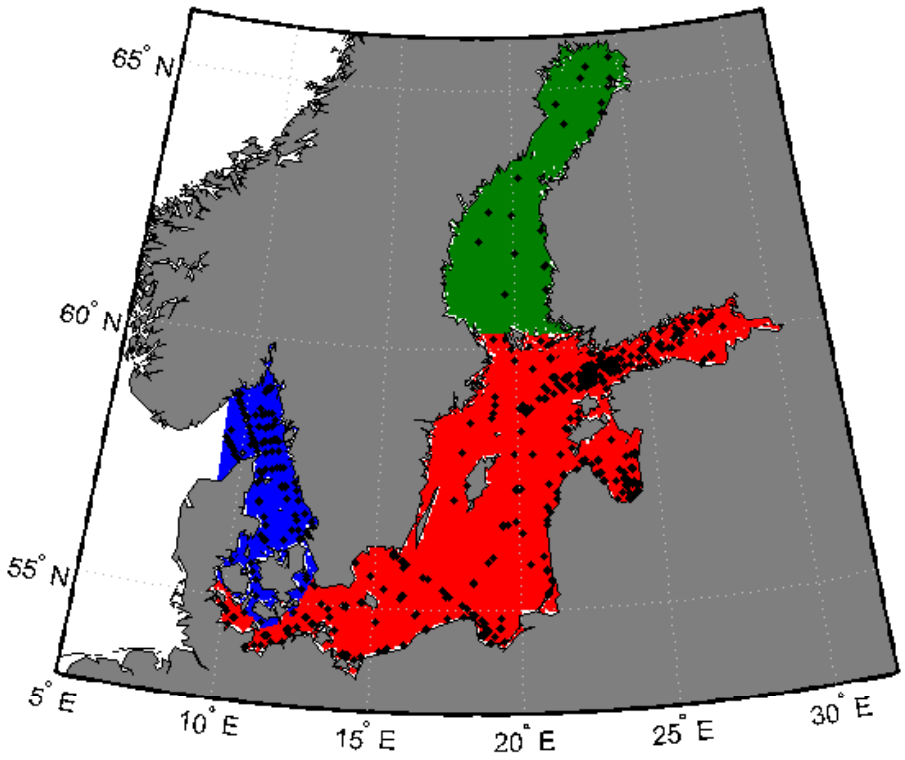

Figure 1. Spatial domain of this work. Blue: Skagerrak and Kattegat. Red: central Baltic. Green: Gulf of Bothnia. Black: in situ stations used in matchup with OC4v6 (N = 4492, see Sect. 3.1).

OSD
12, 2283–2313, 2015

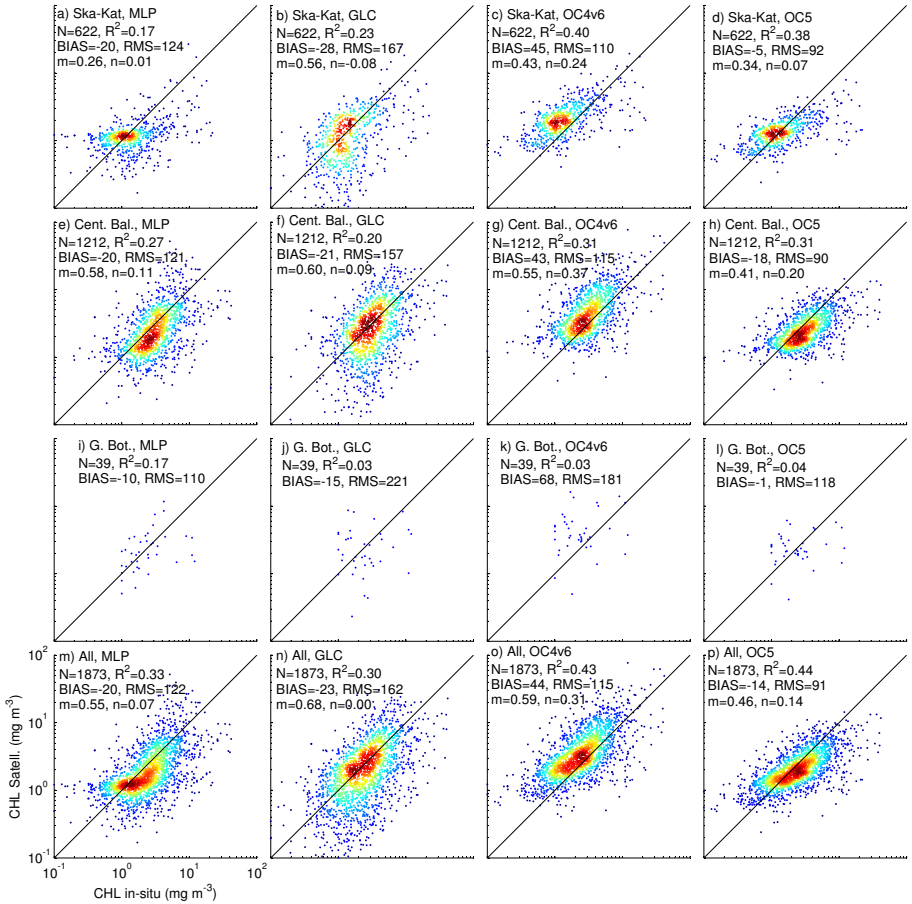

Figure 2. Density scatter plots of in situ vs. satellite-retrieved CHL for all algorithms coinciding. The dashed line of equal value is superimposed. Related statistics are also shown.

OSD
12, 2283–2313, 2015

Remote sensing of chlorophyll in the Baltic Sea

J. Pitarch et al.

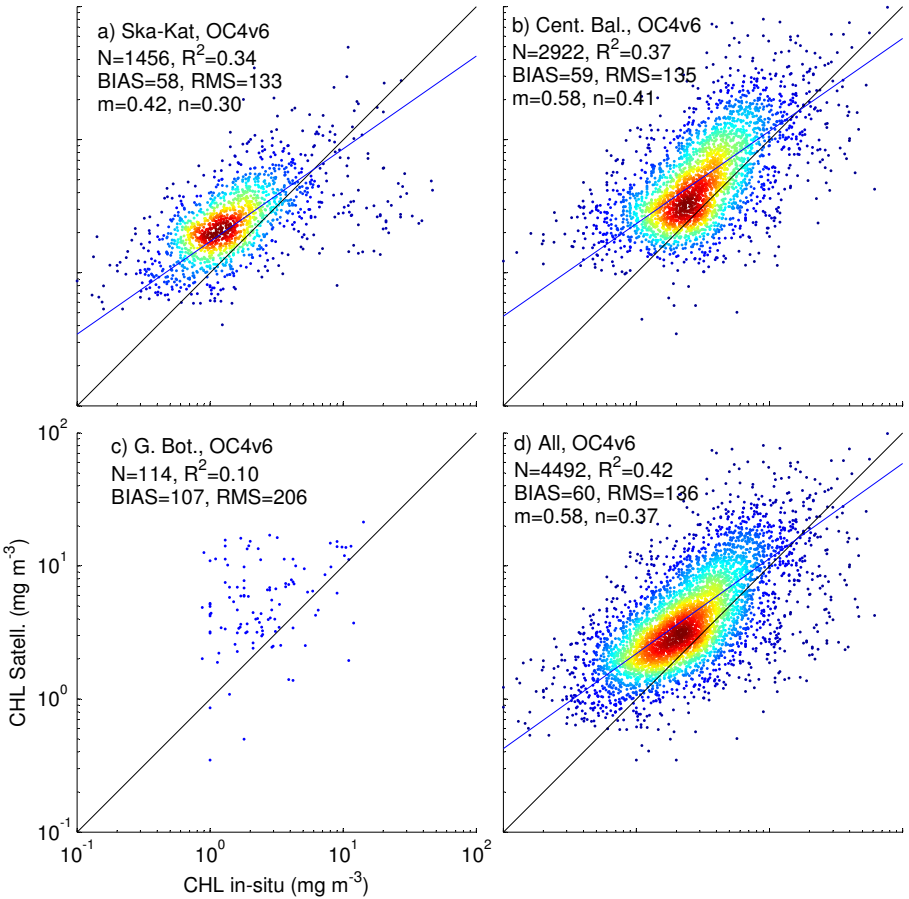

Figure 3. Density scatter plots of in situ vs. satellite-retrieved CHL for OC4v6 algorithm. The best linear regression (solid, blue) and the line of equal value (dashed, black) are superimposed. Related statistics are also shown.

OSD
12, 2283–2313, 2015

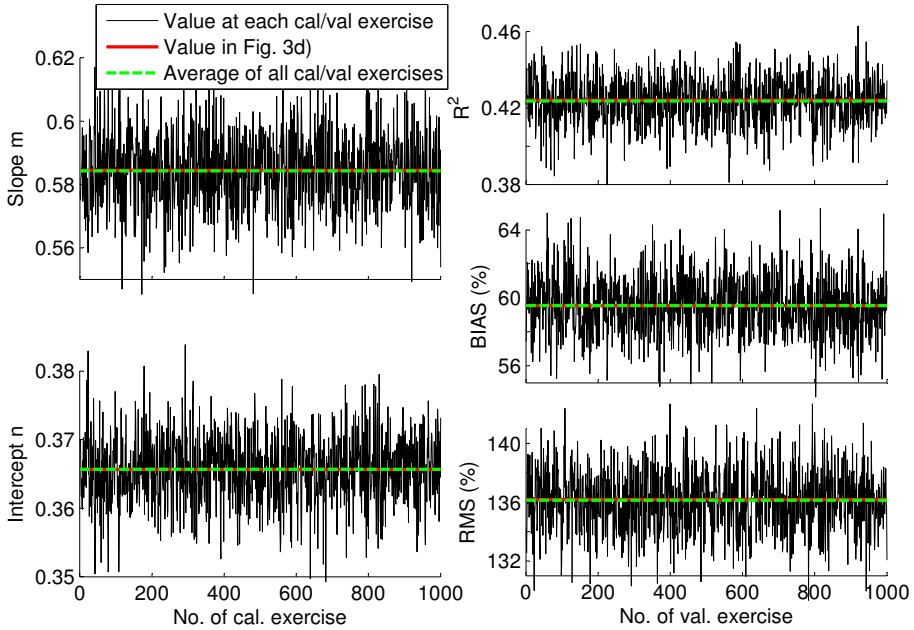

Figure 4. Left, in black: best linear fits (slope and intercept) of 1000 randomly chosen calibration datasets (N_{cal} = 2246) of $\log_{10}$ ($CHL_{in\ situ}$) vs. $\log_{10}$ (CHL_{OC4v6}). In red, slope and intercept (m, n) for the whole dataset, Fig. 3d. In green, average of the 1000 calibration results. Right, in black: statistics when applying each (m, n) pair to the left side to the complementary validation datasets (N_{val} = 2246). These are: coefficient of determination, BIAS (Eq. 1) and RMS (Eq. 2). In red: same statistics found for the whole dataset, Fig. 3d. In green, average of the 1000 validation results.

OSD
12, 2283–2313, 2015

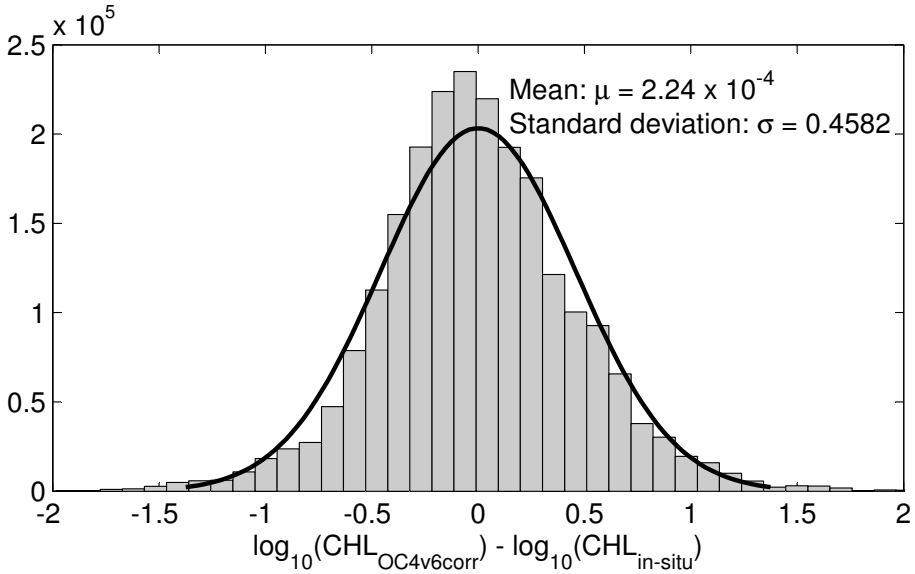

Figure 5. Histogram of the absolute error between $OC4v6_{corr}$ and in situ CHL, both in logarithmic form. Superimposed black line: fitted Gaussian. Associated mean and standard deviation are also shown.

OSD
12, 2283–2313, 2015

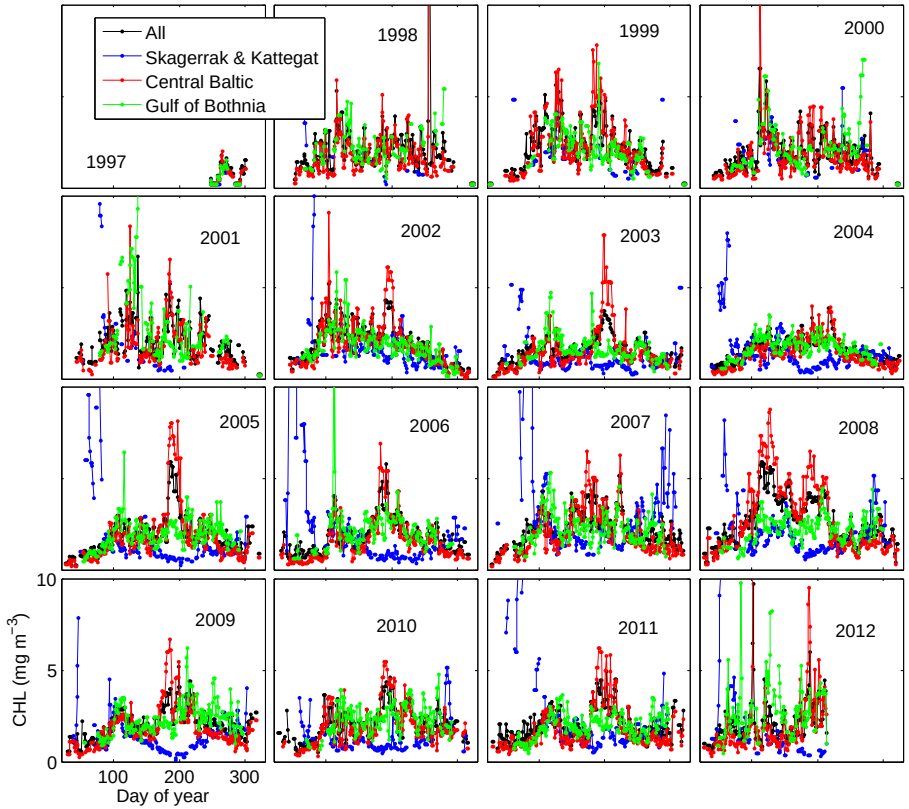

Figure 6. CHL basin averages. The same horizontal and vertical scales apply for all plots in this figure. Full size plots of individual years can be found in the Supplement.

OSD
12, 2283–2313, 2015

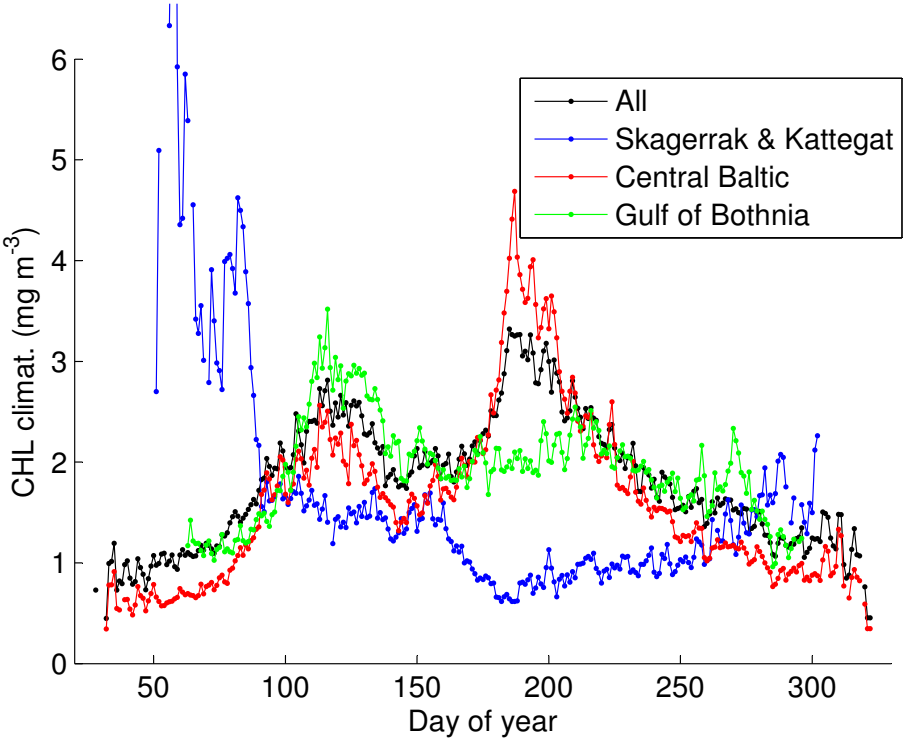

Figure 7. Climatologic CHL (annual averages). Plots of individual time series with their associated standard deviation bars can be found in the Supplement.

OSD
12, 2283–2313, 2015

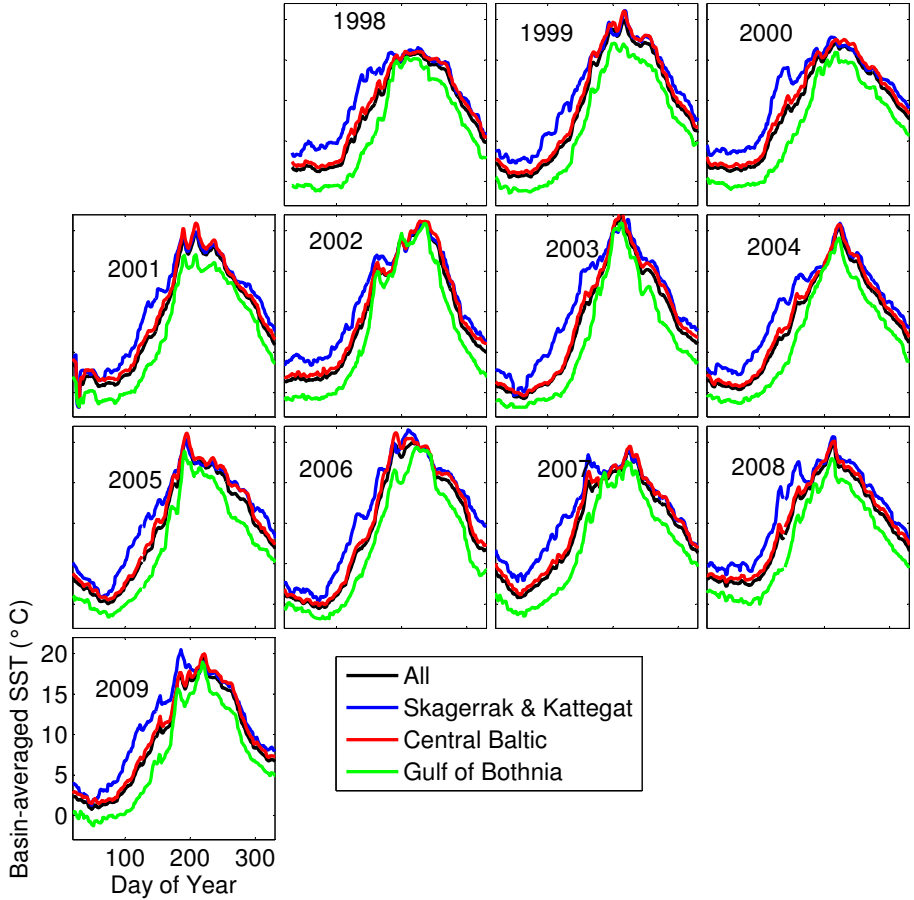

Figure 8. Basin-averaged SST.

OSD
12, 2283–2313, 2015

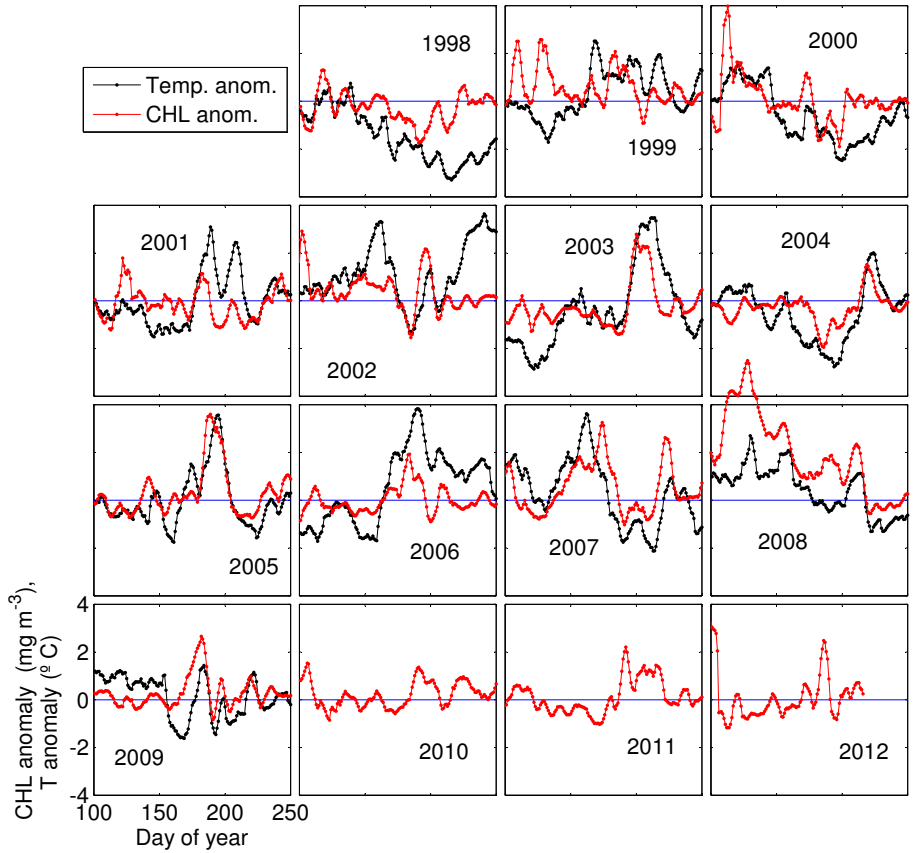

Figure 9. Anomalies of CHL and SST over climatologies at the Central Baltic. The reference value 0 is also displayed. Full size plots of individual years can be found in the Supplement.

OSD
12, 2283–2313, 2015